



Received on 20 June, 2014; received in revised form, 21 August, 2014; accepted, 29 October, 2014; published 01 February, 2015

EVENTUAL IMMUNOLOGICAL BENEFIT OF PHOSPHODIESTERASE IV INHIBITOR (ROLIPRAM) ON THE LUNG AND LENS AFFECTION INDUCED BY SELENIUM IN RATS: A PHARMACOLOGICAL, LIGHT AND SCANNING ELECTRON MICROSCOPE STUDY

Omnyah A. El-Kharashi ^{*1} and Abeer A. Abd El Samad ²

Departments of Pharmacology ¹ and Histology ², Faculty of Medicine, Ain Shams University, Egypt

Keywords:

Selenium; rolipram;
NF kappa B; cataract; bronchitis

Correspondence to Author:

Omnyah A. El-Kharashi

Pharmacology Department
Faculty of medicine
Ain shams university, Egypt

E-mail: omnyah2011@gmail.com

ABSTRACT: The association between chronic bronchitis and cataract is debating. While some referred it to the corticosteroid therapy commonly prescribed to bronchitis, other named different immunological pathways that may be involved in this relationship. We tried to find out the possible immunological benefit of phosphodiesterase IV inhibition in these two common associated conditions. The rats were divided into 4 groups; I: control , II: Selenium (Se), III: roliprampretreated and IV: rolipram post treated groups. Lenses and lung tissues were collected by the end of 2nd week. Upper lobe of right lungs was used to calculate the wet/dry ratios. Histological examinations using H&E, Mallory's trichrome, Proliferation cell nuclear antigen (PCNA) and nuclear factor (NF) Kappa B immunohistochemistry study of the lung were done. Scanning electron microscope and H&E studies of lenses were performed. The lung showed significant (P<0.05) elevation of wet/dry ratios with Se administration. There was infiltration by inflammatory cells, congested blood vessels with thickened wall, collagen fibers were increased (P<0.05) with intense NF-Kappa B immuno-reaction. Moreover, there was increase in PCNA +ve immune-reactive nuclei. All these changes were improved (P<0.05) with rolipram administration. Regarding the lens, rolipram prevented the cortical pathological changes induced by Se. The use of rolipram before Se was more effective in preventing the pathological changes. Rolipram prevented the lens opacity and pulmonary inflammation induced by selenium in rats.


INTRODUCTION: In (2000), Delcourt ¹ and his colleagues found that there is a relationship between asthma or chronic bronchitis and increase the cataract surgery. Searching about the mechanisms involved in both pathological disorders, it seems like that the potential pathways involved in epithelial mesenchymal transition (EMT), may be implicated in this relationship.

EMT has been categorized into 3 types - developmental (Type I), fibrosis and wound healing (Type II), and cancer (Type III).

EMT was first described in early 1980s because of its pivotal role during embryonic development and later because of its implication in the physiological response to injury². However, in pathological contexts such as in tumors or during the development of organ fibrosis, this healing response adopts a threatening nature, steering these diseases towards metastasis and organ failure.

Importantly, the chronic inflammatory microenvironment common to fibrotic and cancer cells emerges as a decisive factor in the induction of the pathological EMT³.

The loss of cell-cell contacts may be the first step of EMT and involves the functional inactivation of the cell-cell adhesion molecule E-cadherin. Repression of E-cadherin expression by the transcription factor Snail is a central event during the loss of epithelial phenotype. Akt kinase activation is frequent in human carcinomas, and

<p>QUICK RESPONSE CODE</p> 	<p>DOI: 10.13040/IJPSR.0975-8232.6(2).591-03</p> <hr/> <p>Article can be accessed online on: www.ijpsr.com</p> <hr/> <p>DOI link: http://dx.doi.org/10.13040/IJPSR.0975-8232.6(2).591-03</p>
-----------------------------------------------------------------------------------------------------------------------	---------------------------------------------------------------------------------------------------------------------------------------------------------------------------------------------------------------------------------------------------------------------------------------------------------------------

Akt regulates various cellular mechanisms including EMT. It was shown that Snail activation and consequent repression of E-cadherin may depend on AKT-mediated nuclear factor-kappaB (NF-kappaB) activation, and that NF-kappaB induces Snail expression and T helper differentiation. Expression of the NF-kappaB subunit p65 is sufficient for EMT induction, validating this signaling module during EMT⁴.

EMT is thought to be involved in the pathogenesis of several chronic lung conditions (asthma, COPD, bronchiolitis obliterans syndrome and lung fibrosis)⁵. Moreover, EMT of lens epithelial cells (LECs) into myofibroblasts is a common association with atopic cataracts⁶. Selenium induced cataract is an established model of cataract in rats⁷ and in rat model of pulmonary hyper-reactivity, low Se status resulted in lower asthma compared to adequate selenium⁸.

In this study we will try to find if the inhibition of NF- kappa B by using a phosphodiesterase (PDE) IV inhibitor (rolipram) inhibits the lung and lens changes in atopic state induced by selenium toxicity or not.

MATERIAL AND METHODS:

Experimental animals:

All animal procedures were done according to recommendations of the Institutional Animal Ethics Committee for Ain Shams University, Faculty of Medicine. Male Wistar rats (weighing 150 to 200 g) purchased from National Research Institute (Cairo, Egypt) were housed in an animal room with temperature (22 °C) and lighting (12 h light–dark cycle) control. An adaptation period of 1 week was allowed before initiation of the experimental protocol.

Chemicals & drugs: Rolipram and Selenium were purchased from Sigma- Chemical Co., Cairo, Egypt.

Experimental procedures

Induction of host immune responses using selenium: To induce lung and lens immune reaction; single dose of selenium 1.5mg /kg body weight was injected subcutaneous (SC)⁹.

Study design

Twenty-four male adults Wistar rats were divided into 4 groups, 6 animals each:

- **Group I:** control group; received single SC injection of 1ml saline and daily i.p injection of 1ml saline for 2 weeks.
- **Group II:** Se group; received single dose of selenium (dissolved in sterile saline) 1.5mg /kg body weight SC and received saline (the vehicle of the rolipram) i.p after 24 h.
- **Group III:** rolipram pre-treated group; received 3mg/kg/d body weight of rolipram (dissolved in sterile saline) i.p 24 h before selenium administration and continued daily for end of the experiment.
- **Group IV:** rolipram post-treated group; received 3mg/kg/d body weight of rolipram i.p 24 h after Se administration and continued daily for end of the experiment.

Measurement of lung wet-to-dry ratio:

The rats were anesthetized using intraperitoneal injection of sodium pentobarbital (50 mg/kg b.w.). The upper lobe of the right lung was taken out for detecting wet/dry weight ratio. Moisture and blood on the tissue surfaces were dried with absorbent filter paper. Then electronic balance was used to weigh the wet tissues immediately and dry weight was measured after the tissues were dried in an 60 °C oven for 96 hours. Finally, the wet/dry weight ratio (W/D) of the lung was calculated¹⁰.

Histological and immunohistochemical studies:

Light microscopic study: The right lung specimens were immediately excised and cut into small samples and fixed in 10% buffered formalin. The lens specimens were excised and remained as a whole; the right one was fixed in 10% buffered formalin to be used for light microscopic study. After fixation, specimens were processed and cut into 5 micron-thick sections.

The lens sections were stained by H&E. The lung sections were stained by H&E, Mallory's trichrome and immunohistochemically by proliferating cell nuclear antigen (PCNA) antibody and nuclear factor- kappa B (NF-Kappa B) antibody (both were ready to use solutions using 2 drops (for 1 hour, from Neo Markers, Lab Vision, CA, USA). Secondary antibody was applied to sections (for 30

min, from DAKO, Denmark). The reaction was developed with DAB solution (for 10 min, from DAKO, Denmark). Finally, the slides were counterstained with Mayer's hematoxylin. Negative controls were processed according to the same protocol, except for the use of the primary antibody¹¹.

Scanning microscopic study: The left lens specimens were rinsed in 2.5% glutaraldehyde fixative solution buffered with 0.1% phosphate buffer for 24 hours. Specimens were then post-fixed in osmium tetroxide for 15 minutes. Then specimens were rinsed in liquid nitrogen in a stainless steel plate where they were surface cracked by a chisel to achieve a clear smooth surface.

The tissues were then dehydrated through ascending grades of ethanol and then were dried at critical point dryer using liquid carbon dioxide with Bal-Tec CPD030. The tissue were further mounted on brass studs with aluminum conducting tape and coated with gold in Bal-Tec SCD005. Specimens were examined with Philips XL30 scanning electron microscope operated at 10 – 30KV, at the electron microscopy unit, Faculty of Medicine, Ain Shams University¹².

Morphometric study: Ten fields of two serial lung sections of all animals were examined using image analyzer Leica Q win V.3 program installed on a computer connected to Leica DM2500 microscope (Wetzlar, Germany) present in Histology Department, Faculty of Medicine, Ain Shams University.

The following parameters were measured: the thickness of the inter-alveolar septum in H&E-stained sections using X20 power lens, the area percent (%) of collagen fibers in Mallory's trichrome-stained sections using X20 power lens, the number of proliferation cell nuclear antigen (PCNA) positive cells / HPF using X40 power lens and the color intensity of NF-Kappa B immuno-reactivity using X20 power lens.

Statistical analysis: Statistical analysis was carried out using Graph pad prism, software program, version 5.0 (2007), Inc., CA, USA. All values were expressed as means \pm standard error of mean. One

way Analysis of variance (ANOVA) for comparison of the different groups was used with significance set at $p < 0.05$. A significant ANOVA was followed by a Tukey's test for multiple comparisons between groups.

RESULTS:

Histological results

Light microscopic and morphometric results of lung:

The H&E-stained sections of group I showed the normal lung architecture with bronchi, bronchioles, alveoli, alveolar sacs and blood vessels. The inter-alveolar septa showed thin portion and thick portions. The alveoli appeared as patent irregular air spaces lined by flat squamous type I pneumocytes and large cuboidal type II pneumocytes (Figs. 1A and 1B). The sections of group II showed severe infiltration by inflammatory cells in inter-alveolar septa, around vessels and in the lumen of most of air spaces. Most of lung alveoli appeared obliterated. Blood vessels appeared congested with thickened walls (Figs. 2A and 2B). Sections of group III showed preservation of lung tissue in spite of selenium treatment, as they appeared more or less similar to group I (Figs. 3A and 3B). Group IV sections showed minimal protective effect of lung tissue as large number of alveoli appeared obliterated with thick inter-alveolar septa. Hemorrhage and inflammatory cellular infiltration appeared in most areas of lung tissue with congested blood vessels (Figs. 4A and 4B). The morphometric study revealed significant increase in thickness of inter-alveolar septa in group II as well as group IV compared to group I and in group IV compared to group III. While the group III showed significant decrease in thickness compared to group II (Table 1).

Mallory's trichrome stained the collagen fibers as they appeared few and fine in group I (Fig. 5). Whereas in group II, collagen fibers were significantly increased (increase collagen fibers area %) compared to group I (Fig. 6, Table 1). Sections of group III showed significant decrease in collagen fibers content and area % than that of group II (Fig. 7, Table 1). Group IV showed significant increase in collagen fibers area % compared to group I and group III, but with

significant decrease in area % of collagen fibers compared to group II (Fig. 8, Table 1).

The sections of group I stained by PCNA antibody showed few numbers of proliferative cells lining the alveoli and in inter-alveolar septa (Fig. 9). These proliferative cells were significantly increased in group II (Fig. 10, Table 1). Sections of group III showed significant decrease in number of proliferative cells compared to group II (Fig. 11, Table 1). Group IV sections showed significant increase in number of proliferative cells compared to group I and group III with significant decrease compared to group II (Fig. 12, Table 1).

Stained sections by NF-Kappa B antibody in group I showed negative immuno-reactivity (Fig. 13). Intense immuno-reaction was seen in lung tissue of group II (Fig. 14). The sections of group III showed minimal increase in immune-reaction intensity of NF-Kappa B (Fig. 15) which was significantly decreased compared to group II (Table 1). As well as in group IV, immuno-reaction intensity was moderately increase (Fig. 16) which was significantly decreased compared to group II and significantly increased compared to group III (Table 1).

Light microscopic results of lens

In the group I, the H and E-stained sections showed that the longitudinally-cut deep mature cortical lens fibers appeared elongated non-nucleated acidophilic and closely packed (Fig. 17). In group II, the lens fibers showed wide gaps in-between (Fig. 18). The sections of group III showed small gaps in-between the lens fibers (Fig. 19). While the sections of group IV showed wide gaps in-between the lens fibers comparable to group II (Fig. 20).

Scanning electron microscopic results of lens

The longitudinal lens fibers of group I appeared compact together (Fig. 21A) and their lateral sides showed the normal structure of ball and socket junctions between them (Fig. 21B). In group II, wide gaps appeared between lens fibers (Fig. 22A) with loss of ball and socket junctions (Fig. 22B). The sections of group III showed more or less normal longitudinal and transverse cut sections of lens fibers (Fig. 23A) with normal ball and socket junctions between them (Fig. 23B). Whereas, the sections of group IV showed narrow gaps in-between the lens fibers with minimal ball and socket junctions between them (Figs. 24A & 24B).

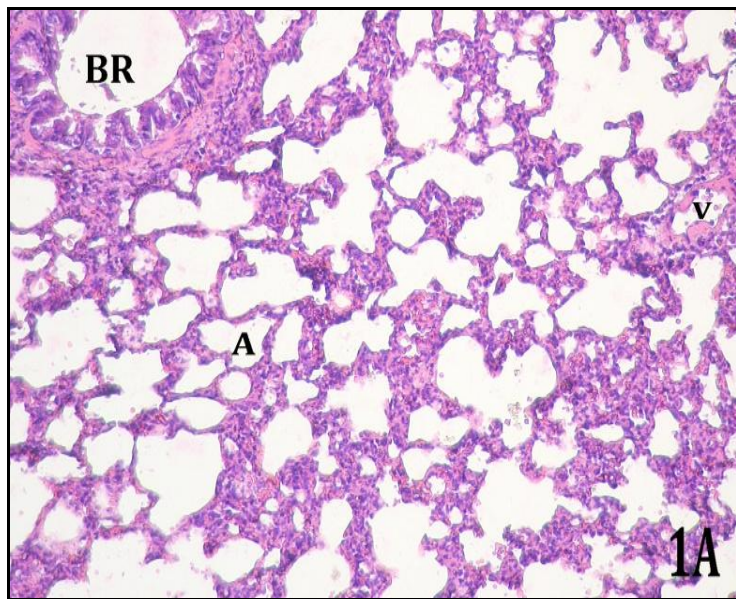


FIG. 1A: SHOWING NORMAL LUNG ARCHITECTURE OF GROUP I INCLUDING A BRONCHUS (BR), ALVEOLI (A) AND BLOOD VESSELS (V). H&E X 140

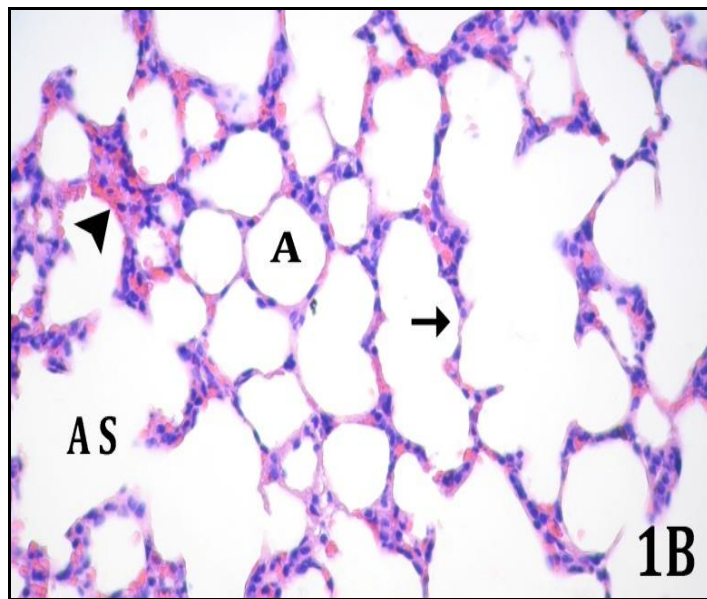


FIG. 1B: SHOWING THE NORMAL ALVEOLAR AIR SPACES OF GROUP I AS ALVEOLI (A) AND ALVEOLAR SACS (A S) WITH THE INTER-ALVEOLAR SEPTA, THE THICK PORTION (▲) AND THE THIN PORTION (†). H&E X 400

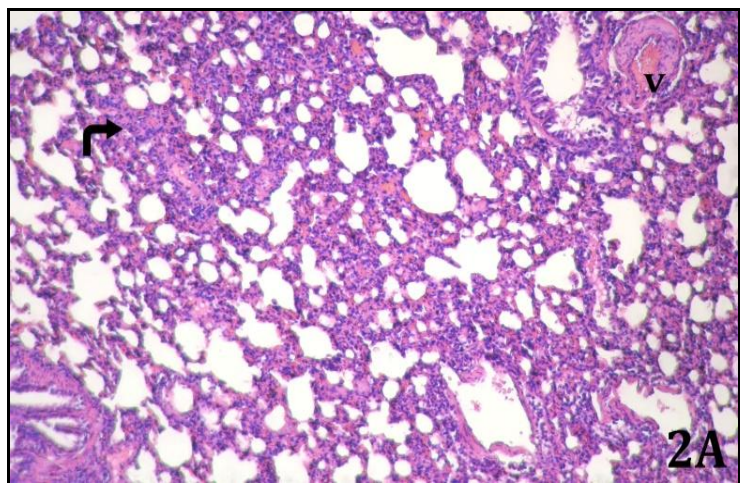


FIG. 2A: SHOWING THE LUNG CHANGES IN GROUP II, OBLITERATION OF ALVEOLI WITH THICKENED INTER-ALVEOLAR SEPTA (CURVED ARROW) AND THICKENED WALL OF BLOOD VESSELS (V). H&E X 140

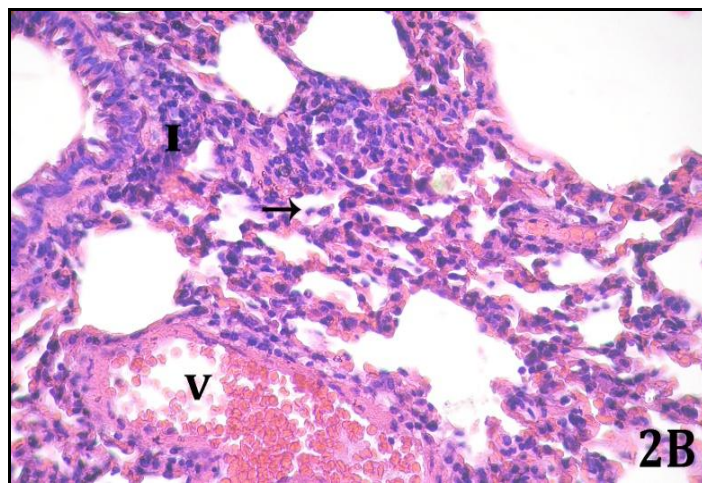


FIG. 2B: SHOWING INFLAMMATORY CELLULAR INFILTRATION (I) AROUND A BRONCHUS AND THICKENED INTER-ALVEOLAR SEPTA WITH HEMORRHAGE IN GROUP II. NOTICE CELLS INFILTRATION IN LUMEN OF ALVEOLI (→) AND CONGESTED BLOOD VESSELS (V). H&E X 400

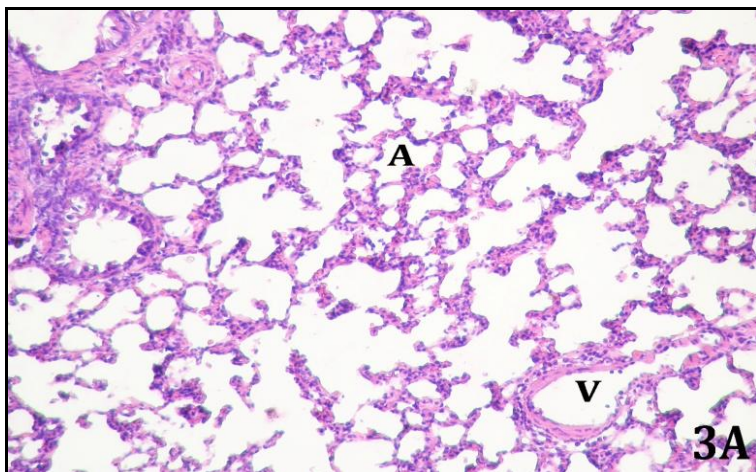


FIG. 3A: SHOWING THAT THE LUNG ARCHITECTURE OF GROUP III IS COMPARABLE TO GROUP I WITH MORE OF LESS NORMAL STRUCTURE OF ALVEOLI (A) AND BLOOD VESSELS (V). H&E X 140

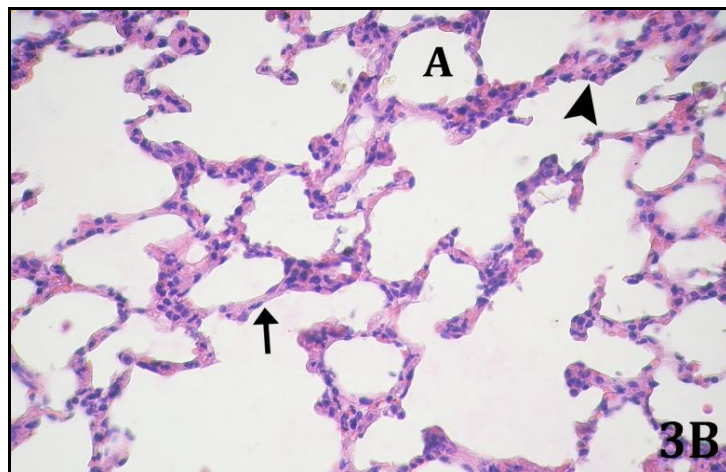


FIG. 3B: SHOWING LUNG ALVEOLI (A) IN GROUP III WITH THE INTER-ALVEOLAR SEPTA, BOTH THE THICK PORTION (▲) AND THE THIN PORTION (↑), COMPARABLE TO GROUP I. H&E X 400

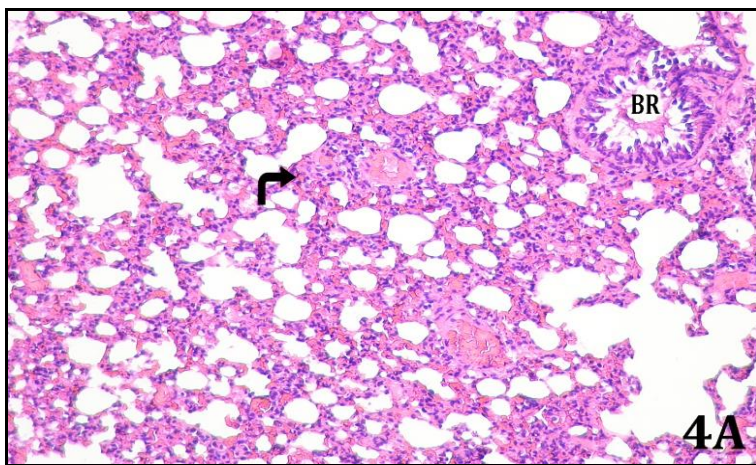


FIG. 4A: SHOWING LUNG ARCHITECTURE OF GROUP IV COMPARABLE TO GROUP II WITH THICKENED INTER-ALVEOLAR SEPTA AND OBLITERATED ALVEOLI (CURVED ARROW). NOTICE EXUDATION AND CELLS INFILTRATION IN A BRONCHUS (BR). H&E X 140

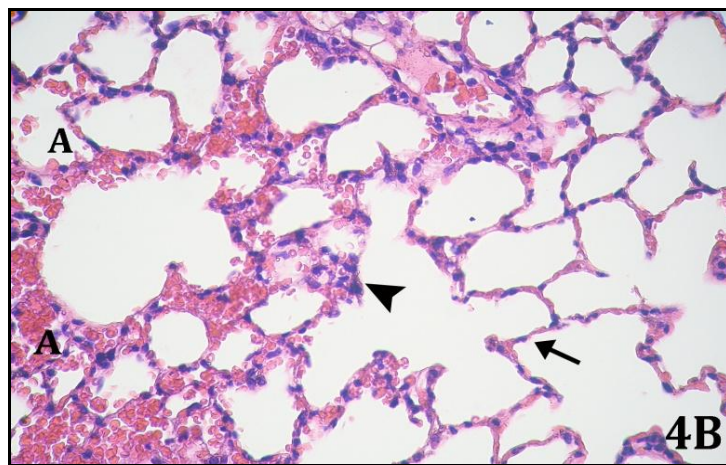


FIG. 4B: SHOWING SOME ALVEOLI (A) WITH RBCS AND INFLAMMATORY CELLS IN THEIR LUMEN IN GROUP IV. OTHER ALVEOLI APPEAR MORE OR LESS NORMAL WITH THICK (▲) AND THIN (↑) PORTIONS OF INTER-ALVEOLAR SEPTA. H&E X 400

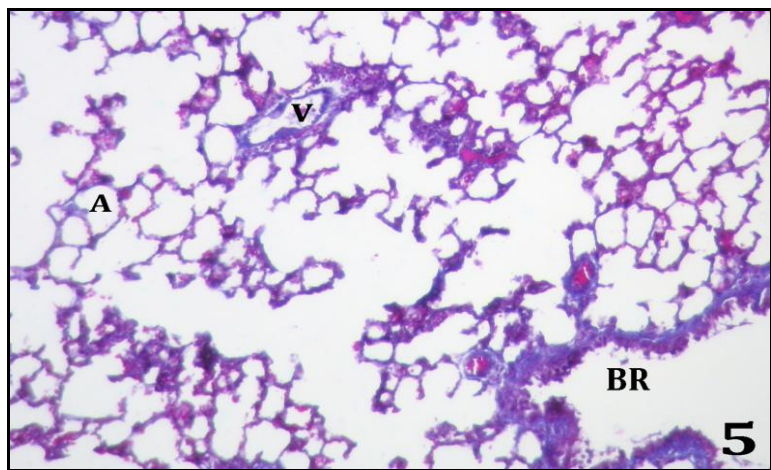


FIG. 5: SHOWING FINE COLLAGEN FIBERS AROUND ALVEOLI (A), BRONCHI (BR) AND BLOOD VESSELS (V) IN CONTROL GROUP. MALLORY'STRICHROME X 140

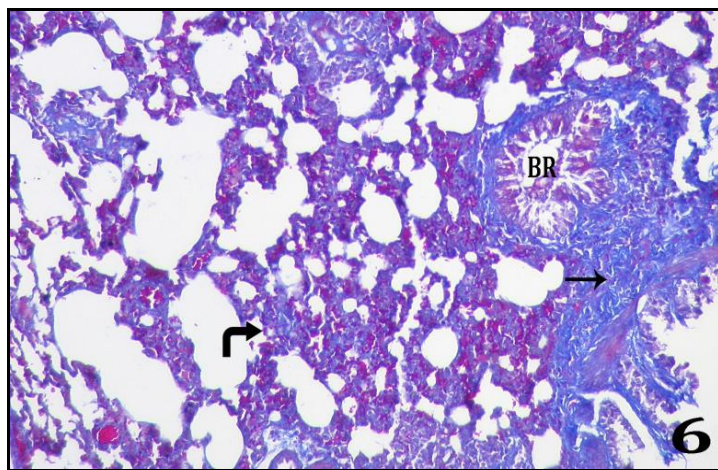


FIG. 6: SHOWING APPARENT SEVERE INCREASE IN COLLAGEN FIBERS (→) AROUND BRONCHI (BR) AND IN THE INTER-ALVEOLAR SEPTA (CURVED ARROW) IN SELENIUM-TREATED GROUP, COMPARED TO CONTROL GROUP. MALLORY'STRICHROME X 140

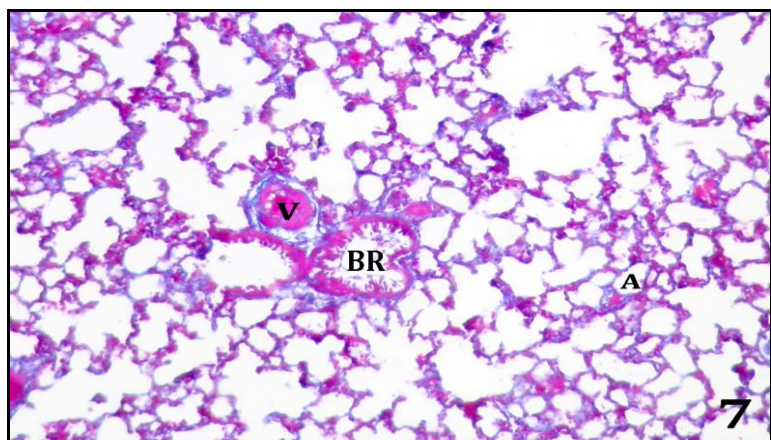


FIG. 7: SHOWING COLLAGEN FIBERS IN R-PRE-TREATED, SELENIUM-TREATED GROUP AROUND BRONCHI (BR), ALVEOLI (A) AND BLOOD VESSELS (V) MORE OR LESS COMPARABLE TO CONTROL GROUP. MALLORY'STRICHROME X 140



FIG. 8: SHOWING APPARENT MODERATE INCREASE OF COLLAGEN FIBERS IN R-POST-TREATED, SELENIUM-TREATED GROUP, COMPARED TO CONTROL GROUP. MALLORY'STRICHROME X 140

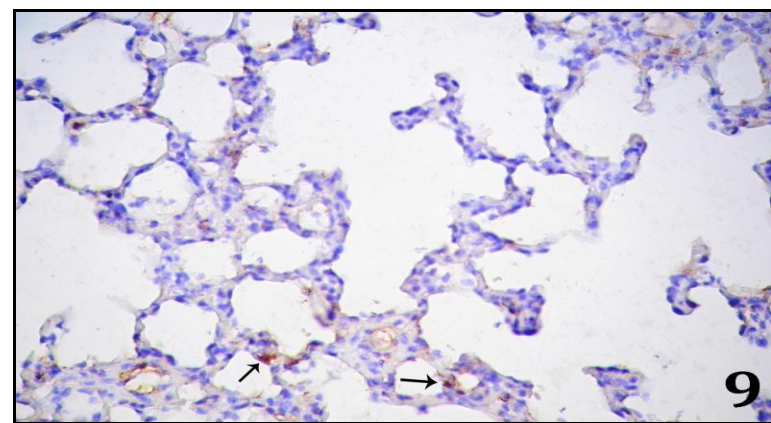


FIG. 9: SHOWING FEW NUCLEI (↑) OF CELLS LINING LUNG ALVEOLI OF CONTROL GROUP WITH +VE BROWNISH IMMUNE-REACTIVITY. PCNA X 400

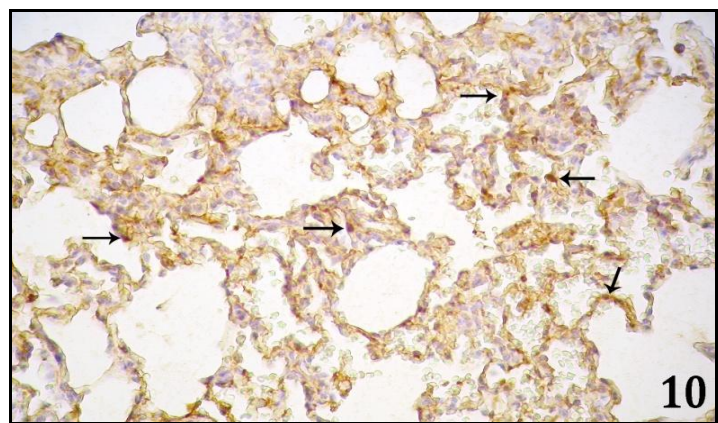


FIG. 10: SHOWING APPARENT SEVERE INCREASE IN NUMBER OF NUCLEI (↑) OF CELLS LINING LUNG ALVEOLI AND IN INTER-ALVEOLAR SEPTA WITH +VE BROWNISH IMMUNE-REACTIVITY IN SELENIUM-TREATED GROUP COMPARED TO CONTROL GROUP. PCNA X 400

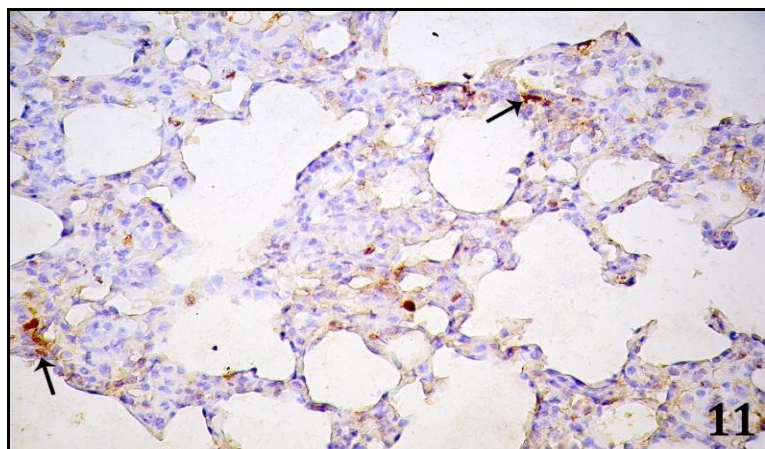


FIG. 11: SHOWING APPARENT MODERATE DECREASE OF NUCLEI (↑) OF CELLS LINING LUNG ALVEOLI AND IN INTER-ALVEOLAR SEPTA WITH +VE BROWNISH IMMUNE-REACTIVITY IN R-PRE-TREATED, SELENIUM-TREATED GROUP, COMPARED TO SELENIUM-TREATED GROUP. PCNA X 400

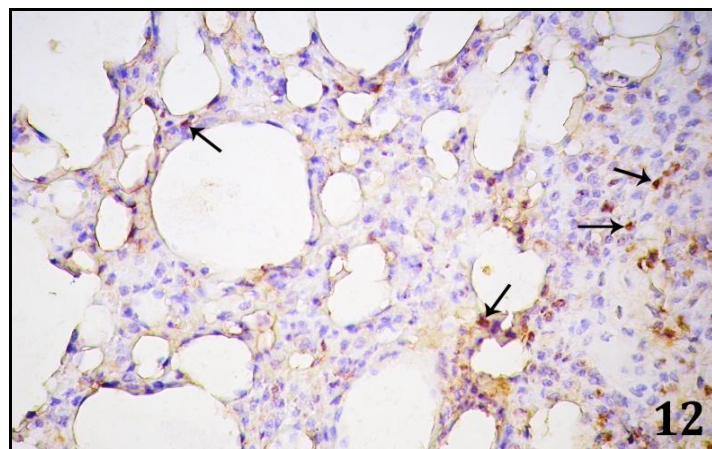


FIG. 12: SHOWING APPARENT MILD DECREASE OF NUCLEI (↑) OF CELLS LINING LUNG ALVEOLI AND IN INTER-ALVEOLAR SEPTA WITH +VE BROWNISH IMMUNE-REACTIVITY IN R-POST-TREATED, SELENIUM-TREATED GROUP, COMPARED TO SELENIUM-TREATED GROUP. PCNA X 400

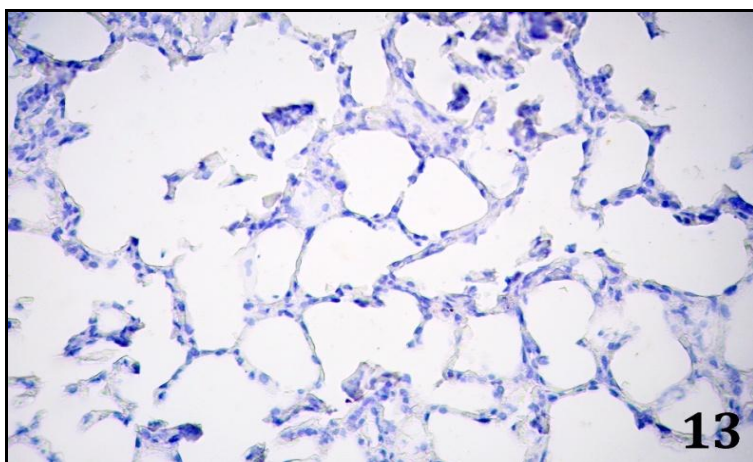


FIG. 13: SHOWING NO IMMUNO-REACTIVITY FOR NF-KAPPA B IN MOST AREAS OF LUNG IN CONTROL GROUP. NF-KB X 400

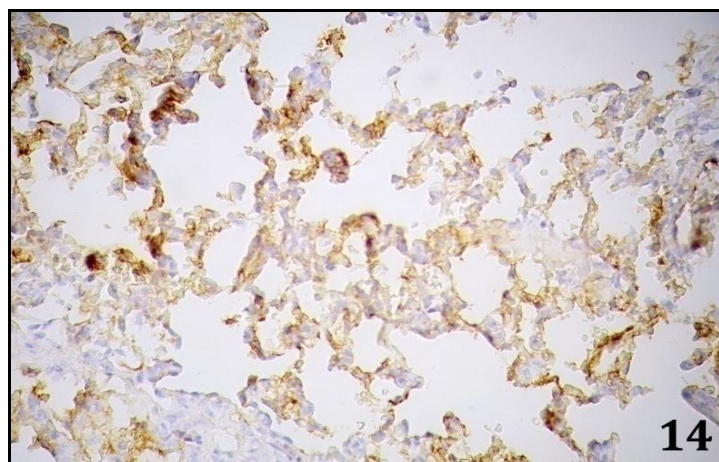


FIG. 14: SHOWING APPARENT SEVERE INCREASE OF IMMUNO-REACTIVITY FOR NF-KAPPA B IN LUNG OF SELENIUM-TREATED GROUP, COMPARED TO CONTROL GROUP. NF-KB X 400

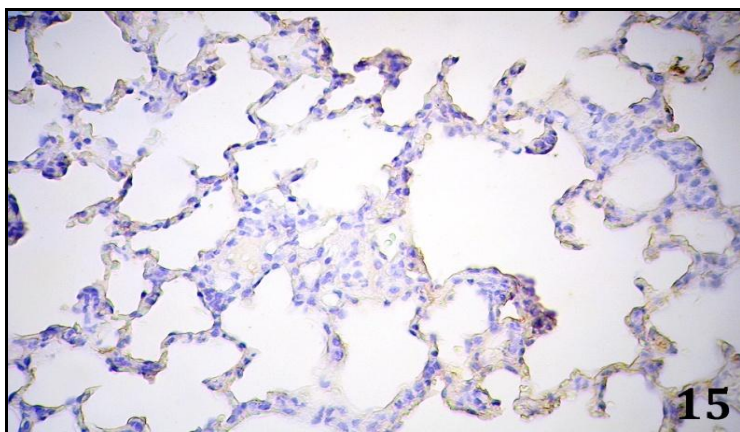


FIG. 15: SHOWING APPARENT MINIMAL IMMUNO-REACTIVITY FOR NF-KAPPA B IN MOST AREAS OF LUNG IN R-PRE-TREATED, SELENIUM-TREATED GROUP, COMPARED TO CONTROL GROUP. NF-KB X 400

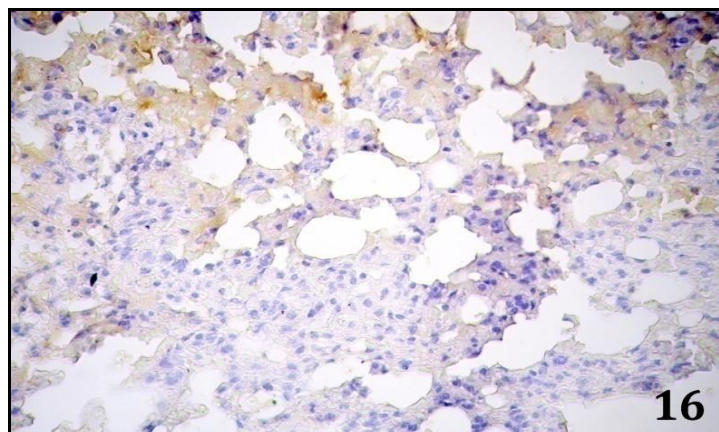


FIG. 16: SHOWING MODERATE IMMUNO-REACTIVITY FOR NF-KAPPA B IN MOST AREAS OF LUNG IN R-POST-TREATED, SELENIUM-TREATED GROUP, COMPARED TO CONTROL GROUP. NF-KB X 400

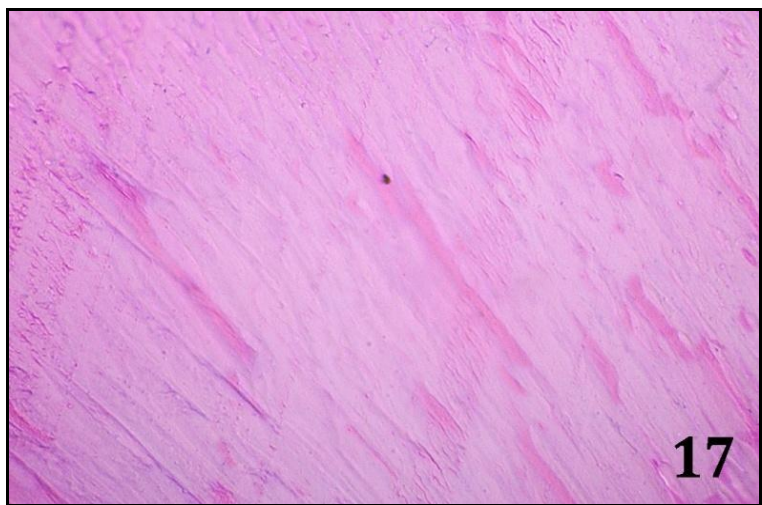


FIG. 17: SHOWING LONGITUDINAL NON-NUCLEATED LENS FIBERS ADJACENT TO EACH OTHER IN CONTROL GROUP. H&E X 400

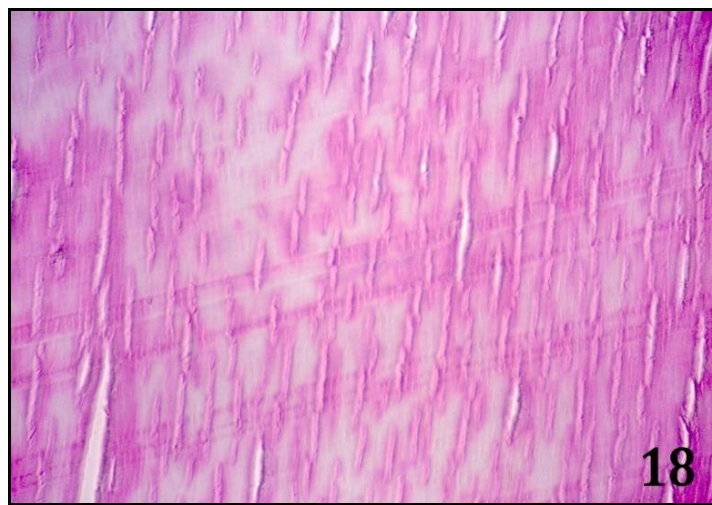


FIG. 18: SHOWING WIDE GAPS BETWEEN LONGITUDINAL LENS FIBERS IN SELENIUM-TREATED GROUP. H&E X 400

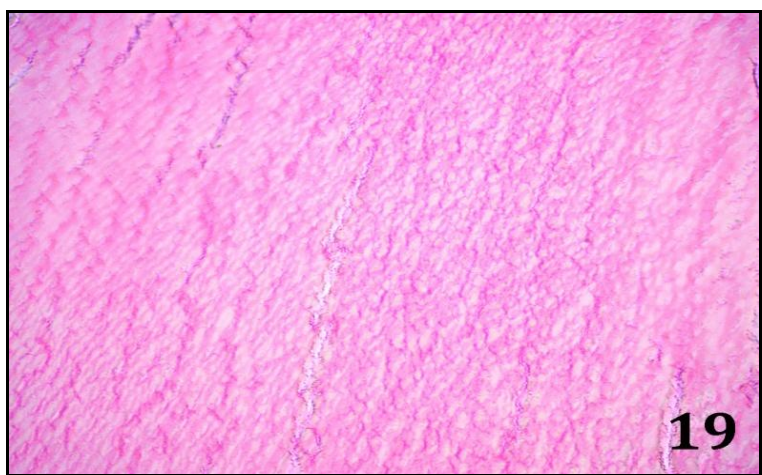


FIG. 19: SHOWING LONGITUDINAL LENS FIBERS WITH SMALL GAPING IN-BETWEEN IN R-PRE-TREATED, SELENIUM-TREATED GROUP. H&E X 400

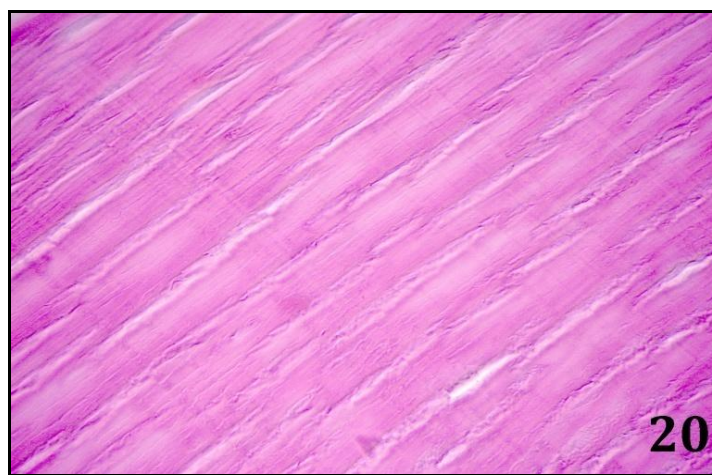


FIG. 20: SHOWING WIDE GAPS BETWEEN LONGITUDINAL LENS FIBERS IN R-POST-TREATED, SELENIUM-TREATED GROUP, COMPARABLE TO SELENIUM-TREATED GROUP. H&E X 400

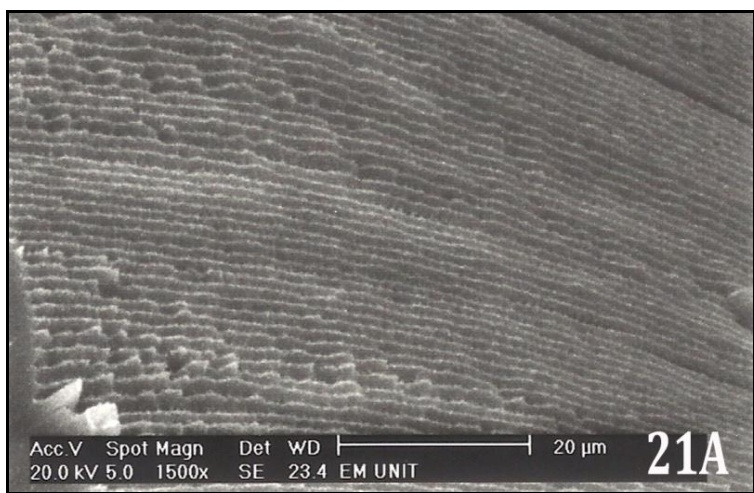


FIG. 21A: SHOWING NORMAL ARRANGEMENT OF LONGITUDINAL LENS FIBERS IN CONTROL GROUP. SEM X 1500

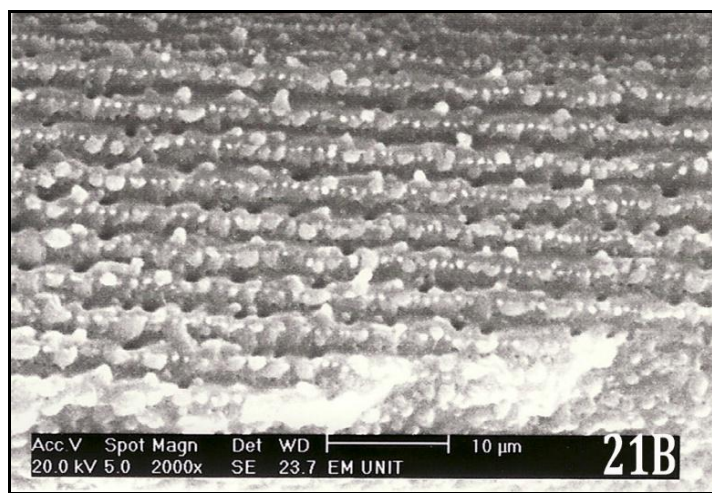


FIG. 21B: SHOWING NORMAL STRUCTURE OF BALL AND SOCKET JUNCTIONS BETWEEN LENS FIBERS IN CONTROL GROUP. SEM X 2000

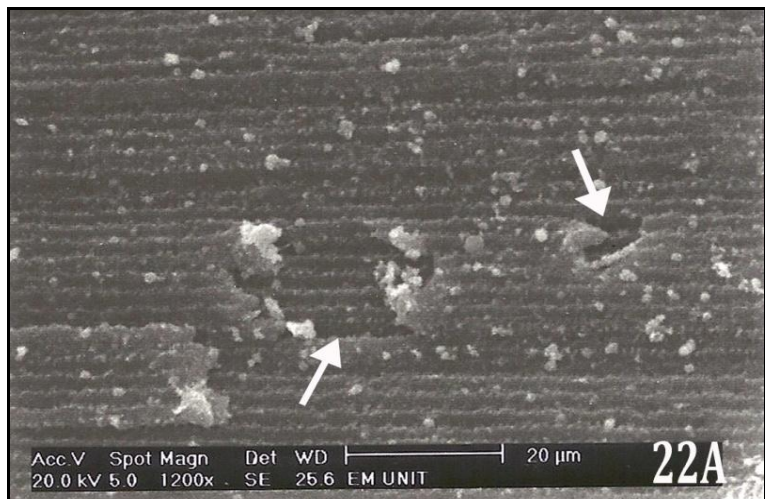


FIG. 22A: SHOWING WIDE GAPS (↑) BETWEEN LONGITUDINAL LENS FIBERS IN SELENIUM-TREATED GROUP. SEM X 1200

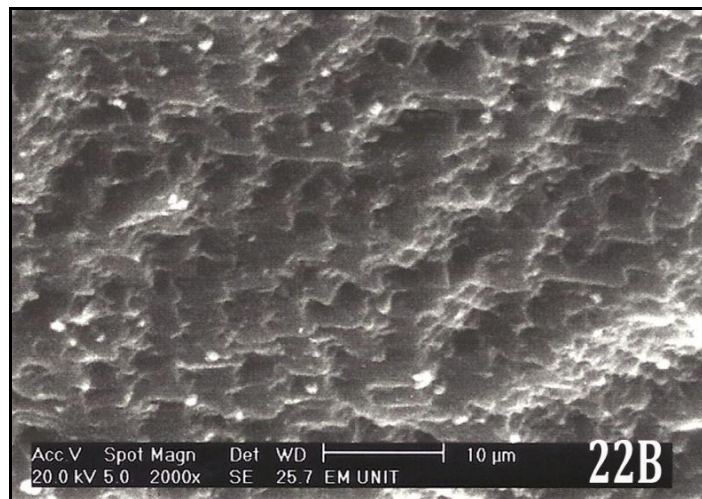


FIG. 22B: SHOWING LOSS OF NORMAL BALL AND SOCKET JUNCTIONS BETWEEN ADJACENT LENS FIBERS WITH GAPS IN-BETWEEN IN SELENIUM-TREATED GROUP. SEM X 2000

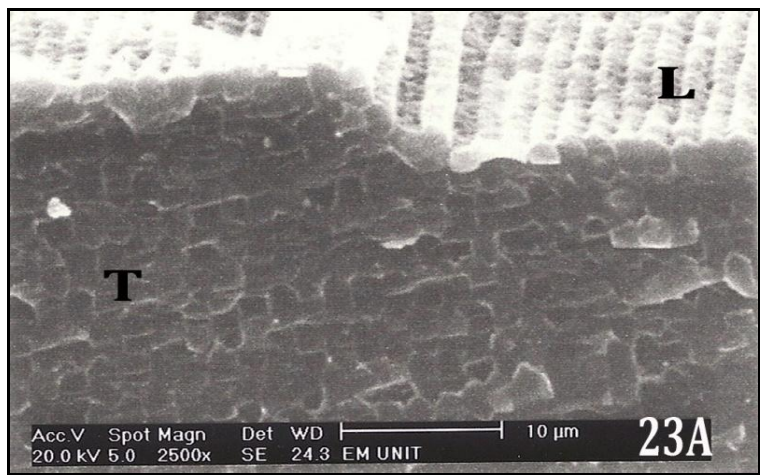


FIG. 23A: SHOWING LONGITUDINAL LENS FIBERS (L) MORE OR LESS COMPARABLE TO CONTROL GROUP WITH HEXAGONAL TRANSVERSELY-CUT (T) LENS FIBERS IN R-PRE-TREATED, SELENIUM-TREATED GROUP. SEM X 2500

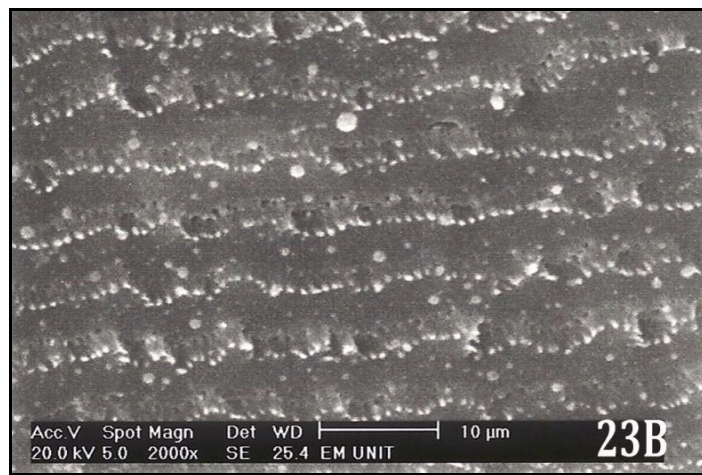


FIG. 23B: SHOWING BALL AND SOCKET APPEARANCE BETWEEN LENS FIBERS IN R-PRE-TREATED, SELENIUM-TREATED GROUP, COMPARABLE TO CONTROL GROUP. SEM X 2000

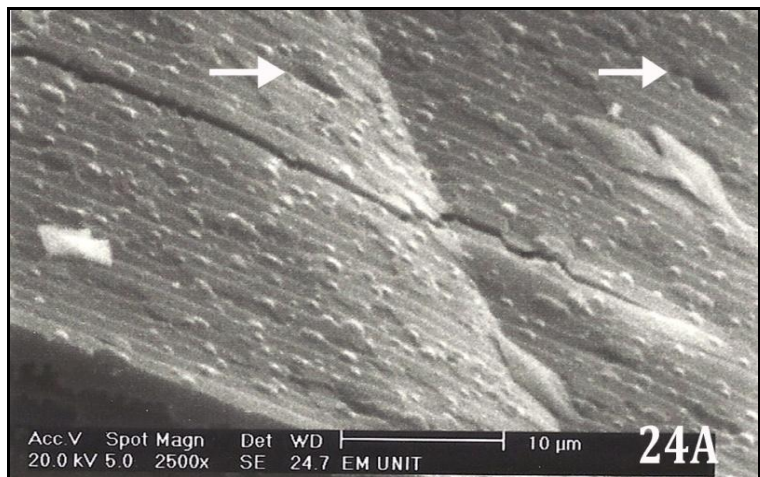


FIG. 24A: SHOWING NARROW GAPS (↑) BETWEEN LONGITUDINAL LENS FIBERS IN R-POST-TREATED, SELENIUM-TREATED GROUP. SEM X 2500

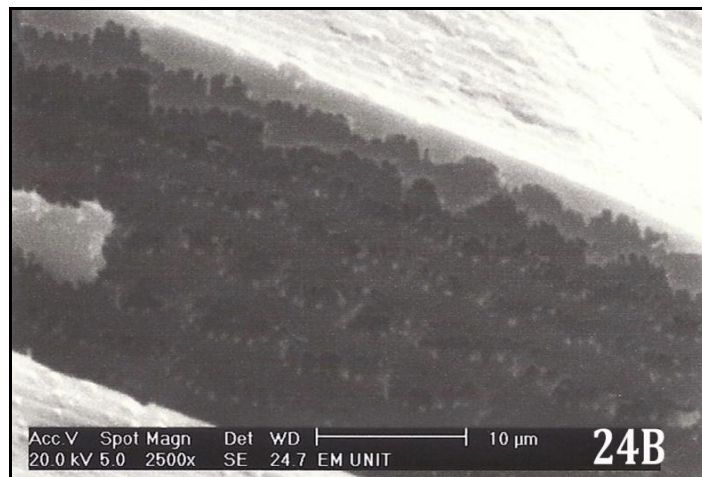


FIG. 24B: SHOWING FEW BALL AND SOCKET JUNCTIONS WITH GAPING BETWEEN ADJACENT LENS FIBERS IN R-POST-TREATED, SELENIUM-TREATED GROUP. SEM X 2500

TABLE (1): SHOWING MEANS ± SEM OF THE MEASURED PARAMETERS IN MORPHOMETRIC STUDY OF ANIMAL LUNGS OF DIFFERENT GROUPS (NUMBER OF RATS IN EACH GROUP =6, NO MORTALITY WAS RECORDED)

GroupsParameters	Group I	Group II	Group III	Group IV
Inter-alveolar septa thickness (µm)	5.59±0.31	27.14±0.84 ^a	7.01±0.42 ^b	18.36±1.05 ^{abc}
Collagen fibers area percentage (%)	8.44±0.95	23.81±0.63 ^a	15.38±0.44 ^{ab}	18.38±0.93 ^{abc}
Number of cells with PCNA +ve immunoreactive nuclei	5.70±0.33	13.05±0.59 ^a	6.70±0.33 ^b	11.45±0.54 ^{abc}
NF-KappaB immunoreaction intensity	0±0 (No immunoreaction)	80.11±0.44 ^a	72.42±0.26 ^{ab}	73.96±0.69 ^{abc}

a = significant to group I (P<0.05)

b = significant to group II (P<0.05)

c = significant to group III (P<0.05)

TABLE 2: WEIGHT LUNG WET/DRY RATIO

Groups	n	Wet/Dry Lung Ratio
Control (group I)	6	4.48 ±0.17
Selenium (Se) (group II)	6	6.55±0.15 ^a
Rolipram pre-treated (group III)	6	4.92±0.06 ^b
Rolipram post-treated (group IV)	6	5.33±0.09 ^{abc}

Values are means ± SEM.

^ap<0.05 compared with control group. ^b p < 0.05 compared with Se group. ^cp<0.05 compared with rolipram pre-treated group.

Effect of rolipram on the wet-to-dry weight ratio (W/D)

Pulmonary edema is a hallmark of selenium toxicity, and the standard assessment of edema is to measure the amount of water in the lungs. Table 2 shows the W/D ratio for the control, Se, rolipram pre-treated and rolipram post-treated groups. The W/D ratio in the Se group was nearly 1.5 times greater than the control group (P <0.05). In the Rolipram groups, the W/D ratio were significantly different compared with those of the Se group, (P <0.05).

DISCUSSIONS: The relationship between chronic bronchitis or asthma and cataract was thought to be due to longstanding use of corticosteroids which will enhance the lens opacification¹. This study tried to find out if there is another theory for the association between inflammatory lung disease and lens opacity that occurs shortly after exposure to selenium (Se). Se is one of metals enriched in ambient air fine particulate matter (PM_{2.5}) thought to contribute to the pathogenesis of PM_{2.5}-induced inflammatory lung diseases¹³ and a powerful and rapid promoter of cataract formation¹⁴. The biological effects of Se are mainly exerted through its incorporation into selenoproteins which are involved in the activation, proliferation and

differentiation of cells that drive innate and adaptive immune responses¹⁵. In the present work, single dose of Se 1.5mg /kg bodyweight was injected subcutaneous. Se-induced inflammation has been widely used to study immune system-mediated tissue injury. The anti-inflammatory activity of rolipram is known¹⁶. This study examined the effect of rolipram before and after exposure to Se on the immunological changes induced in lens and lung tissue.

In this study, Se treated group (group II) showed severe infiltration by inflammatory cells in inter-alveolar septa, around vessels and in the lumens of most of air spaces. Most of lung alveoli appeared obliterated. Blood vessels appeared congested with thickened wall. Using Mallory's trichrome stain, collagen fibers were significantly increased (increase collagen fibers area %) compared to control group (group I) with intense NF-Kappa B immunoreaction, which was seen in lung tissue of group II. The inter-alveolar septa thickness, collagen fibers area percentage, number of cells with PCNA +ve immune-reactive nuclei and wet to dry ratio of the lung were significantly (P<0.05) increased with Se treatment comparing to control group (group I). These results were in accordance with other workers¹⁷.

Se, acting as an oxidant, stimulated the NF-kappa B pathway¹³ resulting in an inflammatory response. The increased expression of NF-kappa B explained the increase inflammatory cellular infiltration and macrophage as well as fibroblasts, which was seen in LM as thickened inter-alveolar septa and increased PCNA-positive cells, resulting in overproduction of collagen and finally leading to lung fibrosis. The explanation of the role of oxidant in lung injury was reported by other investigators working on other models of lung fibrosis¹⁸.

The NF-kappa B has an important role in cell proliferation and differentiation¹⁹ Moreover, Zhang and his colleagues²⁰ tried to explore the correlation between NF-Kappa B activity and cell proliferation in human non small cell lung cancer. They concluded that abnormal NF-Kappa B may be associated with cell proliferation.

Underlying the complicated relationship between Se and pulmonary reactivity is the fact that, while Se affects oxidative stress, Se also exerts a significant influence over the strength of immune responses. In other words, increasing Se may help reduce oxidative stress in the lungs, but it may also boost immune responses to allergens by increasing T helper (Th) responses²¹. Potnis¹² studied the mechanism by which exposure to Se, at environmentally relevant concentrations, leads to an increased release of chemokines by cultured human lung epithelial cells (A549).

They tested the hypothesis that NF-kappa B signaling pathway is involved in the metal induced IL-8 and MCP-1 release by Se. Exposure to Se induced an enhanced release of chemokines at 6 and 24 h, and mediated nuclear translocation of NF- kappa B. Overall, results indicate that Se possess the potential for inducing lung inflammation via an oxidative stress pathway in lung epithelial cells.

Cataract can be considered an illness with a low grade inflammatory status. It is known that inflammation is characterized by oxidative reactions and generation of high oxygen reactive species. Also, the negative correlations between plasma total thiols and globulins represent an argument for a relation between inflammation (high

globulins) and the plasma antioxidant defense (consumption of plasma thiols).

In this work, the lens fibers in Se treated group showed wide gaps in-between. Using scanned electron microscope study, wide gaps appeared between lens fibers with loss of ball and socket appearing junctions. Palmquist²², Padmaja and Raju⁷ results are consistent with our results and they explained that by the pro-oxidant generating free radicals potential of Se at high concentration. Another explanation of Se-induced cataract might be due to permeation of water to the lens fibers as a result of disturbance in the epithelial cell membrane permeability and this interrupted normal fiber synthesis²³.

In the present work, rolipram 3mg/kg body wt. p injection improved the inflammatory picture of lung and cataract formation when administered before Se more significantly than when administered after Se. The inter-alveolar septa thickness, collagen fibers area percentage, number of cells with PCNA +ve immune-reactive nuclei, immuno-reaction intensity for NF-Kappa B and wet to dry ratio of the lung were significantly ($P < 0.05$) decreased with rolipram administration comparing to Se treated group (group II).

The data obtained from Nejman-Gryz²⁴ indicated that rolipram was effective in reducing the rise of lung resistance during early asthmatic reaction (EAR), restricted influx of eosinophils to bronchoalveolar space between 1, 5 and 24 hours after provocation, and reduced increase of histamine concentration in bronchoalveolar lavage fluid (BALf). The inhibitory activity of PDE4 inhibitors against antigen-induced bronchoconstriction may be related to their synergism with endogenous catecholamines to suppress mast cell degranulation²⁵

Blockade of PDE4 with rolipram reduced the production of tumor necrosis factor (TNF)-alpha, interleukin (IL)-5, IL-10, and IL-2. Moreover, they inhibited the activation of NF-kappa B and nuclear factor of activated T cells (NFAT) and stimulated activator protein-1 (AP-1) and cAMP response element-binding proteins (CREBs)²⁶. Thus, the data of this work indicate that blockade of PDE4 with rolipram regulates transcription of a particular

cytokine through inhibition of NF-kappaB that may protect against Se induced tissue injury.

Beta-adrenergic receptor activation of adenylate cyclase was important for rolipramant inflammatory activity since beta blockade abrogated arachidonic acid-induced inflammation. Thus, the antiinflammatory profile of rolipram is unique and may result from inhibition of PMN function and perhaps vasoactive amine release and leukotriene biosynthesis. These actions may be dependent upon endogenous beta-adrenergic activity and are likely mediated through inhibition of PDE IV¹⁶

In the present work, rolipram prevented the lens histological and electron microscopic changes induced by Se. Selenium induced inflammation *per se* or as a ROS-dependent mediator is a connecting link between cataract and oxidative insult. In 2004, Chi and his colleges²⁷ studied the effect of rolipram on uveitis induced by lipopolysaccharide (LPS) in rats. They noted that NF- kappa B translocation and expression of E-selectin, TNF- α , and IL-6 are involved in the pathogenesis of LPS-induced uveitis and are inhibited by rolipram. The inhibitory effect of rolipram in uveitis may be independent of inducible nitric oxide synthase (iNOS) synthesis.

Accordingly, it can be concluded that PDE IV inhibition by rolipram may prevent the lung and lens injury induced by exposure to selenium. There are many pathways that involved in this immunological benefit of rolipram, one of them may be due to inhibition of NF Kappa B pathway. Further experimental study to investigate the effect of rolipram with different doses of selenium on lung, lens and other tissues is recommended.

ACKNOWLEDGEMENT: We want to express our thanks to Dr. Youssef Shoukry (Lecturer of Anatomy, Faculty of Medicine, Ain Shams University) who helped us in the electron microscopic examination done in the Anatomy Department, Faculty of Medicine, Ain Shams University.

COMPETING INTERESTS: Conflict of interest declared none.

REFERENCES:

1. Delcourt C, Cristol JP, Tessier F, Léger CL, Michel F, Papoz L. Risk factors for cortical, nuclear, and posterior subcapsular cataracts: the POLA study. *Pathologies Oculaires Liées à l'Age. Am J Epidemiol* 2000; 1; 151(5):497-504.
2. Cano C, Motoo Y, and Iovanna JL. Epithelial-to-Mesenchymal Transition in Pancreatic Adenocarcinoma . *The Scientific World Journal* 2010; 10, 1947–57
3. López-Novoa JM, Nieto MA. Inflammation and EMT: an alliance towards organ fibrosis and cancer progression. *EMBO Mol Med.* 2009 Sep;1(6-7):303-14
4. Julien S, Puig I, Caretti E, Bonaventure J, Nelles L, van Roy F, Dargemont C, de Herreros AG, Bellacosa A, Larue L. Activation of NF-kappaB by Aktupregulates Snail expression and induces epithelium mesenchyme transition. *Oncogene* 2007; 22; 26(53):7445-56.
5. Bartis DR, Mise N, Mahida RY, Eickelberg O, Thickett DR. Epithelial–mesenchymal transition in lung development and disease: does it exist and is it important? *Thorax* 2013.
6. Hori K, Matsuda A, Ebihara N, Imai K, Mori K, Funaki T, Watanabe Y, Nakatani S, Okada K, Matsuo O, Murakami A. Involvement of plasminogen activator inhibitor-1 in the pathogenesis of atopic cataracts. *Invest Ophthalmol Vis Sci.*2012; 53(4):1846-51
7. Padmaja S., Raju TN. Protective Effect Of Curcumin During Selenium Induced Toxicity On Dehydrogenases In Hepatic Tissue. *Indian J Physiol Pharmacol* 2005; 49 (1) ,111–14
8. Robert L. Norton and Peter R. Hoffmann. Selenium and asthma. *Mol Aspects Med.* 2012 February; 33(1): 98–106.
9. Ostádalová I, Babický A, Obenberger J. Cataractogenic and lethal effect of selenite in rats during postnatal ontogenesis. *Physiol Bohemoslov.*1979; 28(5):393-7.
10. Zhang HL., Liu YF., Luo X., Tan WH., Huang L. Saturated hydrogen saline protects the lung against oxygen toxicity. *Undersea Hyperb Med.*2011; 37(3) ,185-92
11. Bancroft J., Gamble M. Theory and practice of histological techniques. 6th ed. Churchill Livingstone: Elsevier, 2008; 121-150-433.
12. Shoukry Y. Scanning electron microscopy, a new approach of an old issue. *EJH* 2011; 34, 179: 81.
13. Potnis PA, Mitkus R, Elnabawi A, SquibbK and PowellJL. Role of NF- κ B in the oxidative stress-induced lung inflammatory response to iron and selenium at ambient levels *Toxicol. Res.*2013; 2, 259-69
14. Shearer TR., Anderson RS., Briiron JL. Influence of Selenife and Fourteen Trace Elements on Cataractogenesis in the Rat. *investvophthalmol vis sci.*1983; 24(4), 417-23
15. Huang Z. Rose AH and Hoffmann PR. The Role of Selenium in Inflammation and Immunity: From Molecular Mechanisms to Therapeutic Opportunities. *Antioxid Redox Signal* 2012; 16(7), 705–43
16. Griswold DE., Webb EF., Breton J., White JR., Marshall PJ., Torphy TJ. Effect of selective phosphodiesterase type IV inhibitor, rolipram, on fluid and cellular phases of inflammatory response. *Inflammation* 1993;17(3), 333-44
17. Cherdwongchareonsuk D., Águas AP., Henrique R., Upatham S., Sousa Pereira A. Toxic effects of selenium inhalation: acute damage of the respiratory system of mice *Hum Exp Toxicol.*2003; 22 (10), 551-7
18. Zhao J., Shi W , Wang YL, Chen H, Bringas P Jr., Datto MB., Frederick JP., Wang XF., Warburton D. Smad3 deficiency attenuates bleomycin-induced pulmonary

- fibrosis in mice. *Am J Physiology Lung Cell MolPhysiol* 2002; 282 (3), 585-93.
19. Li X and Stark GR. NF κ B-dependent signaling pathways. *Exp Hematol*. 2002; 30(4), 285-96.
 20. Zhang J., Xu J., Zhang ZX, DU CL., QuaoLF., Ni W., Chen SX. Nuclear factor- κ B activity and its correlation with cell proliferation in non-small cell lung cancer tissues. *ZhonghuaJie He He Hu Xi ZaZhi* 2007; 30(10), 771-5
 21. Hoffmann PR. Selenium and asthma: a complex relationship. *Allergy*. 2008; 63, 854-6
 22. Palmquist BM., Fagerholm P., Landau I. Selenium-induced cataract--a correlation of dry mass content and light scattering. *Exp Eye Res*. 1986; 42(1), 35-42.
 23. Anderson RS. Trune DR., Shearer TR. Histologic Changes in Selenite Cortical Cataract. *Invest Ophthalmol Vis Sci* 1988; 29(9), 1418-27.
 24. Nejman-Gryz P., Grubek-Jaworska H., Glapiński J., Chazan R. Effect of phosphodiesterase 4 inhibitor (rolipram) on experimental allergic asthma-guinea pig model. *Pneumonol Alergol Pol* 2006; 74(1), 106-12.
 25. Underwood Dc. Matthews Jk, Osborn Rr, Bochnowicz S, Torphy Tj. The Influence of Endogenous Catecholamines on the Inhibitory Effects of Rolipram against Early- And Late-Phase Response to Antigen in the Guinea Pig. *J Pharmacol. Exp Ther* 1997; 280(1), 210-9
 26. Jimenez JI, Punzon C, Navarro J, Munoz-Fernandez Ma, And Fresno M. Phosphodiesterase 4 Inhibitors Prevent Cytokine Secretion by T Lymphocytes by Inhibiting Nuclear Factor- κ B and Nuclear Factor of Activated T Cells Activation. *J Pharmacol Exper Ther* 2001; 299 (2):753-9
 27. Chi ZL, Hayasaka S, Zhang XY, Hayasaka Y and Cui HS. Effects of Rolipram, a Selective Inhibitor of Type 4 Phosphodiesterase, on Lipopolysaccharide-Induced Uveitis in Rats. *Invest. Ophthalmol. Vis. Sci* 2004; 45 (8): 2497-502

How to cite this article:

El-Kharashi OA and Abd El Samad AA: Eventual Immunological Benefit of Phosphodiesterase IV Inhibitor (Rolipram) On the Lung and Lens Affection Induced By Selenium in Rats: A Pharmacological, Light and Scanning Electron Microscope Study. *Int J Pharm Sci Res* 2015; 6(2): 591-03. doi: 10.13040/IJPSR.0975-8232.6 (2).591-03.

All © 2013 are reserved by International Journal of Pharmaceutical Sciences and Research. This Journal licensed under a Creative Commons Attribution-NonCommercial-ShareAlike 3.0 Unported License.

This article can be downloaded to **ANDROID OS** based mobile. Scan QR Code using Code/Bar Scanner from your mobile. (Scanners are available on Google Playstore)